Third United Nations
International Conference
on the Peaceful Uses
of Atomic Energy

A/CONF.28/P/373
USSR
May 1964
Original: RUSSIAN

Confidential until official release during Conference

THE CALCULATION OF THE THERMAL UTILIZATION IN CELLS WITH COMPLEX FUEL ELEMENTS

G.A.Bat, E.A.Grigoryeva, V.N.Lebedev , A.I.Prokhorov
L.S. Tzygankov

I.

It seems possible that major errors in the calculation of θ- coefficient of the thermal utilization in the heterogeneous nuclear reactor lattices should be determinedly excluded by means of a transition from a one-velocity diffusion equation to a kinetic equation of thermalization with its rather detailed description of the cross-sections of the introduction between neutrons and chemically bound moderator nuclei in a thermal movement. The research dedicated to this programm has been going on for already a few years and, in fact, are nearing completion now.

Yet, in the cases of numerous calculation versions, those of nuclear fuel burnout included, the overall consideration of kinetic and thermalization effects is extremely cumbersome. This primarily concerns lattices containing not only separate cylindrical fuel elements but rather whole bundles of them or a system of co-axial tubes, in other words, channels, surrounded by a moderator layer which is thicker than thermal neutron free path. This channel structure is typical to the Lenin icebreaker reactor and the reactor MR. The consideration of the channel's geometry and changing of its composition in the course of the burn-out needs calculation programmes whose realisation takes a good many hours of fast computer operation. The necessity then springs up to evolve sipmler methods to ensure satisfacory precision and to rest on reference data obtained in experiments and accurate calculating procedures. It looks feasible for this purpose to tackle the problem in two stages: to determine first of all the space variations of the thermal neutron spectrum form or

else, which is its equivalent, the space dependence of cross-sections and then take up the one-velocity equation with the pre-given law of average cross-sections changes. Furthermore, it makes lots of sense to try the simplest model to calculate the neutron spectrum, for example, the diffusion heavy--gas model (perhaps, with effective moderator parameters), and seek to find an acceptable approximate solution of the thermalization equation. Bearing it in mind that the thermalization correction is commonly 10% as to the value $(1-\theta)$, we may hope to decrease an error by an order in the case of systems without high temperature gradients, free of substances with low energy resonances. The problem's second part for complicated lattices, one cannot obviously do without the kinetic equation to be solved, at least one per a cell, and two or three times at a deep burnout. Thus, the artificial means of the type of the Amouyal - Benoist-Gorowitz integral method are practically out of the question. Expansion into spherical harmonics does not necessarily provide the due accuracy, the Monte-Carlo methods are rational only to low symmetry channels (for those, say, of the first atomic power station). The characteristics method (Vladimirov) and Sn-methods (Carlsson) seem most suitable for symmetric cells.

2.

The equation of neutron thermalization in the reactor cell moderator in the space of coordinates and velocities under diffusion approximation (it is supposed the monoatomic heavy gas model) assumes the form:

$$D\Delta f(\bar{r},v)+\frac{1}{v^2}\frac{\partial}{\partial v}\left[\frac{\xi\Sigma_s}{2}\cdot\frac{kT_{cp}}{m}v^3\frac{\partial f}{\partial v}+\frac{\xi\Sigma_s}{2}v^4 f\right]-v^{\circ}\Sigma_c^{\circ}f+v^2Q_0(v)=0. \qquad (1)$$

Here $f(\bar{r},V)$ is the neutron density in the space of coordinates and velocities;

$\Sigma_s, D=(3\Sigma_{tr})^{-1}, v^{\circ}\Sigma_c^{\circ}$ - are ordinary macroscopic constants, which are said to be independent of the velocity V;

T_m - temperature of a moderator in $^{\circ}K$, K - the constant of Boltzman, m - mass of neutron, ξ -average logarythmic

373

energy decrement per collision; v^0 - the most probable velocity for the Maxwellian spectrum of the temperature T_m ; $Q_0(v)$ - neutron source.

Let us multiply equation (I) by $v^2 dv$ and integrate for all the velocities . Aware of the behavior of f at $V=0$ and ∞ , obtain:

$$D\Delta\Phi(\bar{r}) - v^0\Sigma_c^0 N(\bar{r}) + q = 0, \qquad (2)$$

where $N(\bar{r}) = \int_0^\infty v^2 f(\bar{r},v)\,dv$, $\Phi(\bar{r}) = \int_0^\infty v^3 f(\bar{r},v)\,dv$ - are the integral density and the flux of neutrons.

Equation (2) differs from an ordinary one-velocity diffusion equation for thermal neutrons in its second member, which substitutes for the member $(v^0/\bar{v})\Sigma_c^0\Phi(\bar{r})$. Therefore, a necessary suggestion for putting down a one-velocity diffusion equation reads that the neutron integral density $N(\bar{r})$ can be substituted by the ratio $\Phi(r)/\bar{v}$, where $\bar{v}$ - the average velocity for the Maxwellian spectrum of a certain temperature $T_{n.g.}$ independent of the coordinates and ascribed to the neutron distribution. It will be only natural to make here a next step on the suggestion still there about, the Maxwellian type of the neutron spectrum in the cell's moderator, the spectrum temperature being looked upon as a coordinate function. It should be noted that the results of calculations and experimental data both confirm this approximation.

By the multiplication of equation (I) by $v^3 dv$ and integration on all the velocities it is obtained:

$$D\Delta\Psi(\bar{r}) - \frac{\xi\Sigma_s}{2}\Psi + \frac{\xi\Sigma_s}{2}\frac{3kT_m}{m}N(\bar{r}) - v^0\Sigma_c^0\Phi(\bar{r}) + q_1 = 0 \qquad (3)$$

where $\Psi(\bar{r}) = \int_0^\infty v^4 f(\bar{r},v)\,dv$.

Substituting in equation (2), (3) $\Phi(\bar{r})/\bar{v}(\bar{r})$ for $N(r)$ and taking it into account that the spectrum nature flow of neutrons is similar in all the moderator points, the system emerges

$$D\Delta\Phi(\bar{r}) - \frac{v^0}{\bar{v}(\bar{r})}\Sigma_c^0\Phi(\bar{r}) + q = 0, \qquad (4)$$

373

$$D\Delta\Psi(\bar{r})-\frac{\xi\Sigma_s}{2}\Psi+\frac{\xi\Sigma_s}{2}\cdot\frac{3kT_{cp}}{m}\cdot\frac{1}{\bar{v}(\bar{r})}\Phi(\bar{r})-v^{o}\Sigma_c^{o}\Phi(\bar{r})+q_1=0 \qquad (5)$$

$$\bar{v}=\frac{8}{3\pi}\frac{\Psi(\bar{r})}{\Phi(\bar{r})}\,,\qquad \left(\frac{\bar{v}}{v^{o}}\right)^2=\frac{4}{\pi}\,\frac{T_{n.g.}}{T_m} \qquad (6)$$

The relation between the free members q and q_1 is not difficult to get making use, for one, of the well-known result pertaining to the spectra in homogeneous mediums without space gradients:

$$T_{n.g.}\simeq T_m\left[1+K\frac{\Sigma_c^{o}}{\xi\Sigma_s}\right],\qquad K=1{,}84 \qquad (7)$$

and the corresponding solution of the system (4) + (6)

$$T_{n.g.}\simeq T_m\left[1+\frac{4}{3}\left(\frac{q_1}{qv^{o}}-\frac{2}{\sqrt{\pi}}\right)\cdot\frac{\Sigma_c^{o}}{\xi\Sigma_s}\right]\,.$$

This brings $q_1 = 2{,}508\ qv^{o}$.

The boundary conditions on the cells' S_c cuter surface are apparent:

$$\nabla\Phi\big|_{S_c}=\nabla\Psi\big|_{S_c}=0 \qquad (8)$$

Once within the fuel block there are no light nuclei and the exchange of energy between neutrons and nuclei is non-existent, the purely diffusion boundary conditions on the surface of the cylindrical block section and moderator R_o can read as follows:

$$D\frac{\nabla\Phi}{\Phi}\Big|_{R_0}=2\left[\frac{m}{2kT_{n.g.}(R_0)}\right]^2\int_0^{\infty}\frac{D_o}{L_o}\frac{I_1}{I_o}\left(\frac{R_o}{L_o}\right)v^3\exp\left[-\frac{mv^2}{2kT_{n.g.}(R_0)}\right]dv, \qquad (9)$$

$$D\frac{\nabla\Psi}{\Psi}\Big|_{R_o}=\frac{8}{3\sqrt{\pi}}\left[\frac{m}{2kT_{n.g.}(R_o)}\right]^{5/2}\int_0^{\infty}\frac{D_o}{L_o}\frac{I_1}{I_o}\left(\frac{R_o}{L_o}\right)v^4\exp\left[-\frac{mv^2}{2kT_{n.g.}(R_0)}\right]dv, \qquad (10)$$

where $D_o=(3\Sigma_o)^{-1}$, $L_o^2=(3\Sigma_o\Sigma_{oc})^{-1}$, $\Sigma_o=\Sigma_{oc}(v)+\Sigma_{os}$ -usually macroscopic fuel parameters.

Conditions (9) and (10) are easily generalised as to other fuel block geometries.

The above calculation procedure for a neutron thermalization model on the ideal monoatomic gas of heavy nuclei can be applied to real mediums carrying the selection of the effective values of K and D parameters.

Taking into account a very peculiar calculation of the

water moderator it must be borne in mind not only how rough the heavy gas model is, but also the suggestion made: D = const. The corresponding account of the dependence D(v) would cause the change of the equation (4), (5) without giving them the due accuracy. Proceeding from the assumption that in the water medium $D \sim v$ and introducing immediately into the approximate equations two constants D_ψ and $D_\phi = D$ to be considered independent of the coordinates, it is found:

$$\frac{D_\psi}{D_\phi} = \frac{\left[\int_0^\infty x^3 e^{-x^2} dx\right] \cdot \left[\int_0^\infty x^5 e^{-x^2} dx\right]}{\left[\int_0^\infty x^4 e^{x^2} dx\right]^2} = 1{,}132$$

The choice of effective K and D values will be given in section 3. The aproximate solution obtained above of a thermalization equation makes it possible to average the cross-sections of neutron interaction with the cell substances over the energy range and then to solve the one-velocity kinetic problem with the cross-sections dependent on coordinates. It is noteworthy, that there is no implication of the Maxwellian spectrum form within the block whatsoever.

The one-velocity kinetic equation for the neutron distribution function in the cell F is given the form:

$$\bar{\Omega}\nabla F + \Sigma F = \frac{\Sigma_s}{4\pi} \int F(\bar{r}, \bar{\Omega}') g(\mu_0) d\bar{\Omega}' + S(\bar{r}). \qquad (11)$$

Here $\bar{r}$ is the vector-radius of points x, y, z; $\bar{\Omega}$ - a single vector of the neutron velocity direction, $\mu_0 = \cos(\bar{\Omega} \cdot \bar{\Omega}')$; $g(\mu_0)$ is the indicatrix of scattering, $S(\bar{r})$ -is the source of neutrons.

As usual, $\Omega = i\Omega_x + j\Omega_y + k\Omega_z$; $\Omega_x = \sin\vartheta \cdot \cos\varphi$; $\Omega_y = \sin\vartheta \cdot \sin\varphi$; $\Omega_z = \cos\vartheta$, where ϑ -is the angle between $\bar{K}$ and $\bar{\Omega}$, while φ -is the angle between $\bar{i}$ and the projection $\bar{\Omega}$ against the plane x, y.

To solve the equation (II) the method of characteristics has been used [1], [2] and the code has been compiled for a fast computer.

Straight line segments - the paths of neutron constitute the characteristics of the linear differential expression $\Omega\nabla F$. Then the straight line l is chosen in coordinate space, and ζ - parameter is introduced descriptive of the length on l. In the points of the straight line the neutron flux moving in

373

the direction $\vec{\Omega}$, coinciding with l is describable in terms of the equation:

$$\frac{dF}{d\zeta} + \Sigma F = \frac{\Sigma_s}{4\pi} \int F(\bar{r},\bar{\Omega}') g(\mu_0) d\bar{\Omega}' + S(\bar{r}) \cdot \qquad (12)$$

For obtaining the exhausting picture of neutron distribution in the circular cylindrical cell it is sufficient to consider the straight lines l on the planes y = const. and neutrons moving along these straight lines. Indeed, the function F in this case is dependent on the module of projection $\bar{r}$ against the plane x, y,, the angle Θ between the direction of neutron movement and the axis z and the angle ψ between projections $\bar{\tau}$ and Ω against the plane x, y. Apparently, the variation range of these variables is exhausted as long as we move along all the straight lines l.

Let, the characteristics l forms the angle Θ with the axis z, then $d\zeta = (1-\gamma^2)^{-1/2} dx$, where $\gamma = \cos\theta$, and the equation (12) may be written as follows

$$\frac{\partial F(x,y,\gamma)}{\partial x} + \frac{\Sigma}{\sqrt{1-\gamma^2}} F = \frac{1}{\sqrt{1-\gamma^2}} \left[\frac{\Sigma_s}{4\pi} \int F(r,\bar{\Omega}') g(\mu_0) d\bar{\Omega}' + S(r) \right] \qquad (13)$$

The neutron reflection conditions on the cell boundary are looked upon as the boundary conditions for F

$$F(R_1, \mu, \gamma) = F(R_1, -\mu, \gamma), \text{ where} \qquad (14)$$

R_1 is the cell radius,

$$\mu = x/r = \cos\Psi; \quad 0 \le x^2 + y^2 \le R_1^2; \quad 0 \le \gamma \le 1; \quad -1 \le \mu \le 1.$$

It is possible to consider that cross-sections Σ, Σ_s are step constant functions,

and the scattering is linear anisotropic one, that is

$$g(\mu_0) = 1 + 3\mu_0 \bar{\mu}_0,$$

where $\bar{\mu}_0$ represents the average scattering angle cosine. The right part of the equation being expressed (13) through Q, the equation reads as

$$Q = \frac{1}{\sqrt{1-\gamma^2}} \left[\Sigma_s \Phi + 3\bar{\mu}_0 \mu \sqrt{1-\gamma^2}\, \Sigma_s \mathcal{J} + S(r) \right], \qquad (15)$$

$$\Phi = \frac{1}{\pi} \int_{-1}^{+1} \frac{d\mu'}{\sqrt{1-\mu'^2}} \int_0^1 F d\gamma', \quad \mathcal{J} = \frac{1}{\pi} \int_{-1}^{+1} \frac{\mu' d\mu'}{\sqrt{1-\mu'^2}} \int_0^1 \sqrt{1-\gamma'^2}\, F d\gamma'.$$

373

The equation (15) with the condition (11) is convenient to solve by the iteration method [illegible] the predetermined approximate expression for Q. At [illegible], the first approximation contains P_1 - value of [illegible] and J, to come over, however, in the most immediate future to P_3 -solution as the final one for example cell calculation. The ordinary nonhomogenius differential equation of the first order along the characteristic l

$$\frac{\partial F(x,y,\gamma)}{\partial x} + \frac{\Sigma}{\sqrt{1-\gamma^2}} F(x,y,\gamma) = Q \qquad (16)$$

is solved at the fixed y and γ parameter values, F being determined in the cross-points between the characteristic and the straightline X=0 and semi-circumferences $x^2 + y^2 = r_i^2$; $0 \le r_i \le R_1$; $y > 0$.

The variable γ mesh-points find themselves to be the positive roots of the Legandre even polynomials, meanwhile, the spacing on y is not affected by the choice r_i . The solution of the equation (16) calls, above all, for finding $F=F_o$ at the characteristic's left end. For this purpose, in the equalities, which link up the two function values F in meighbouring points on the characteristic, all the F_n are subsequently excluded from as early as F_1. As a result, the relation between F_o and F_n comes about where F_n is the value of F at the right end. The relation, as well as the boundary condition $F_o=F_N$ defines F_o.

For the distribution function integral the formula is taken of the fourth precision order.

Once integrated, the equation (16) along the characteristic within the stretch from point (x_{n-1}, y) to point (x_n, y) yields

$$F(x_n,y,\gamma) - F(x_{n-1},y,\gamma) + \frac{\Sigma}{\sqrt{1-\gamma^2}} \int_{x_{n-1}}^{x_n} F\,dx = \int_{x_{n-1}}^{x_n} Q\,dx , \qquad (17)$$

where

$$\int_{x_{n-1}}^{x_n} F\,dx = \frac{F_n + F_{n-1}}{2} h + \frac{h^2}{12}\left(\frac{\partial F_{n-1}}{\partial x} - \frac{\partial F_n}{\partial x}\right) + O(h^4) \qquad (18)$$

On solving the equation (16) with the right part the cycle resumes as soon as the new value of Q is arrived at. To bring about better convergence the iteration method is used where the major deviation from the exact solution is to be found within the P_1 - approximation, and the L.A. Lusternik method is involved as supplementary one. [3].

The process is ended as soon as the difference of Φ values in any of the cell points for the two forthcoming iterations comes below the given value ε . ε being equal to 10^{-4}, it is sufficient accomplish $\sim$ 15 iterations. The functions F, Φ and $\mathcal{J}$ come to the print. It takes all in all 10 - 15 minutes to calculate the cell.

Up to 128 points along r , 80 point for y and 16 points for γ are allowed.

In further calculations it proved indispensable to use as many as 100 points along the radius, 60 y -points and 5 points for γ . The vicinity of the moderator and absorber section boundaries, that is to say, in the areas of substantial changes of Φ , the radial step was smaller. The spacing for y grows in the absorber, because of the higher flux anisotropy.

It is noteworthy, that the specific one-velocity calculation of a few ring multi-layer cells with a water moderator-the cell study is forth-coming, - was indicative of that the accepted neutron scattering anisotropy count was detailed in excess, and Σ_s is liable to an easy substitution by $\Sigma_{tr} = (1 - \bar{\mu}_o)\Sigma_s$ without any loss of accuracy as is done in the diffusion approximation.

As the reference point in controlling the code the calculation of a double-zone cell was chosen, investigated in the study [4]

Its parameters: $R_o = 1{,}3$ cm, $R_1 = 11{,}28$ cm,
$\Sigma_{oc} = 0{,}3230\ \text{cm}^{-1}$; $\Sigma_o = 0{,}7221\ \text{cm}^{-1}$; $\Sigma_{1c} = 3{,}118 \cdot 10^{-4}\ \text{cm}^{-1}$,
$\Sigma_1 = 0{,}3721\ \text{cm}^{-1}$, $\bar{\mu}_{oo} = \bar{\mu}_{01} = 0$, $S_o = 0$, $S_1 = 1$

The below result of the calculation of the characteristic method ratio $\bar{\Phi}_1 / \bar{\Phi}_0$ is compared with the outcomes of the study (4) (Table I)

It must be borne in mind that the reflection conditions on the cell boundary (14) are not rigorous, provided the water film is thin enough the latter might involve higher values for $\bar{\Phi}/\bar{\Phi}_0$.

373

In the above instance this error does not show through, yet, the results of the following section for the small radius cells are likely be pregnant with the lack of percision.

3.

The thermal utilization, calculation scheme as described in section 2 requires, as mentioned above, the selection of effective values for thermalization parameters K and D.

Fig. I shows the calculation results of neutron gas temperature distribution in the cell[x] with a water moderator and block of the natural uranium, detailed upon in the study by Mostovoy [5] The temperature of the intra-block neutron gas under the conditions of a normmaxwellian form spectrum was understood to be the value of $T_{n.g} = (m v_m^2)/4K$ where V_m the most probable velocity of the distribution $v^2 \cdot n(v)$.

It is common knowledge that the experimentally obtained neutron spectrum was that of neutrons moving parallel to the blocks; therefore as long as $r = 0$ the stars mark down the values obtained by Martchuck, Smelov (etc.)[6] in solving the kinetic thermalization equation for parallel and normal beams and for spectrum which has been averaged in the direction of the neutron flight. It is evident, that the values $K = 1{,}46$ (7) /respectively , $q_1 = 2{,}223\ q\ V^0$ / and $D = 0{,}1561\ \sqrt{T_{n.g.}/294}$ ensure a substantial degree of coincidence of our results with the most reliable information pertaining to the neutron spectrum in this cell.

Instantaneously upon the finding of $T_{n.g.}$ (for the indoor water temperature only) followed the determination of the N(r) - integral density distribution represented in Fig. 2 by the dotted line. The solid line there is a result of the kinetic calculation with the prematurely selected distribution $T_{n.g.}$ (r); the points are the results of the experiments by Stolyarov and al. /8/ obtained by way of copper foil activation. Conscious of the experimental errors outside the drawing, the calculation still looks satisfactory; the diffusion curve proved too sloping as should have been expected.

---

x) The calculation was made of a cell with the set aluminium ... the exact distribution of alluminium being represented in Fig. 2.

373

The "exact" value of θ = 0,7[illegible]; the diffusion calculation gives θ = 0,8007 and, consequently, brings about an error ~ 10% into the ratio Φ/Φ_0

The scheme also underwent testing by the calculation of other geometrically simple uranium-water lattices, among them those with slightly enriched metallic blocks which once were a matter of most close study in the Brookhaven National Laboratory, USA (BNL). Tables II and III quote the typical results for the cases where the "blackness" is nearing the extreme.

It should be remembered that throughout our calculus the use was made of the uranium neutron cross-section system [10], slightly different from that accepted in the Brookhaven laboratory, all the more since the transition to the latter considerably deteriorates the agreement between the experimental and calculation data. It is very likely to be explained by the insesitivity of our calculations toward the position of the upper boundary of the thermal neutron spectrum.

For simple cells "the pre-heating" within the block is practically independent of the lattice step, and the temperature of a cell boundary is approximately desdribed by the simple relation

$$T_{n.g.} = T_m \left[1 + K\left(\frac{\Sigma_c}{\xi \Sigma_s}\right)^{H_2O} / (1-\theta)\right]$$

It is of interest to trace whatever effect different calculation approximations have on the calculated value of θ. Table IV shows an example of this on the [illegible] of cells with rods of 0.600 inch diameter and [illegible] at 1.3% . (See [illegible]).

Clearly, in all the above cases the diffusion approximation error is outweighing although thermalization effect at the large spacing bears ever greater importance.

Thus, the simple cylindrical block calculations confirm the efficiency of this method and set the door open for considering more complicated cells. As an example, the light-water [illegible] have been chosen with fuel channels especially designed for study of uranium-water reactor criticality. The channels [illegible] geometrically complex as well as the whole of the [illegible] core. The channels [illegible] shipping system of two, three or four tubular fuel [illegible] rods being inserted

into each other.

UO_2 with the enrichment of $\sim 20\%$ serve as fuel, the cladding and the channel's jacket tube are made out of stainless steel, the sizes transpire very well from the figures.

Fig. 3. and 4 illustrate the results of an one-velocity calculation for the flux distribution along the three-ring channel cell, as effected in P_1-, P_3 - and kinetic approximations for the real geometry and for single-zone channel model-with cross-sections of the averaged type. In the latter case P_3 - calculation differs from kinetic one so very little that it become possible to chart out a single common line instead of the two curves. Simultaneously, this common curve is vastly different from the distribution not only in the larger absorbtion region but in the moderator as well, provided this distribution is representative of the fine channel structure. In this way, the exact complex cell calculation should be based invariably on the detailed description of its geometry, this description on many occasions appearing more essential than the extensive description of diffusion process. The cases, however few they might be, when by force of accidental occurences the flux for a single zone model looks more or less coinciding with the actual channel flux (Fig.5) the error in θ might be substantial because of a sufficient neutron "depression" by the fuel layers.

It is appropriate to mention that the approximation P_3 turns out to lack correctness so far as it is poorly descriptive of the intra-channel neutron distribution, anyway, for the absorbing layers of the optical thickness $(2_{\Delta r})\ \Sigma_c \simeq 0.5$.

Thus, the saw-like vibrations of the P_3-flux in Fig.3 are about two times less than the exact ones. Fig. 5 is particularly dedicated (henceforth a little exaggerated representation) to the kinetic flux in the rings for the three values Σ_c of ring different from each other by two times; the flux alteration range in this case is almost strictly proportionate to Σ_c of ring.

The comparison between the flux distributions calculated after the scheme under discussion with the fluxes obtained in the suggestion of the neutron spectrum in the cell volume being constant (maxwellian with $T_{neg.} = T_m \left[1 + 1{,}46 \frac{\Sigma_c}{\xi \Sigma_s}\right]$) is given in Fig. 6

Despite the inconsiderable divergence in fluxes the error in θ looks substantially big, it is, above all, due to the difference in the neutron gas temperatures (See Table V).

The fig. 7 is illustrative of that the Fick law for the diffusion $J = -D\nabla\Phi$ provided the solution is exact enough, does not hold even qualitatively, and the number of sign changes of the neutron current curve J is not equal to the number of the extremums of the Φ flux.
However, the diffusion current is by far closer to the exact than is the diffusion flux in relation to the exact flux, that can be helpful in the numerical solution for the calculation of derivatives in the formula (18).

The flux redistribution in the process of the fuel burnout (Fig. 8) leads to a marked change in the absorption ratio in different rings. Thus, if the heating power in the outer ring makes unity the middle and inner ring intensity changes with regard to the data of Table VI.

Clearly, these redistributions must count in choosing the coolant flow rate through the gaps and the burnout calculation simplification must be approached in a very careful manner.

Finally, Fig. 9 - 11 gives the neutron gas temperature distributions and those of neutron fluxes along the cell radius with two, three or four ring channels. One cannot fail to notice that the "pre-heating" in any of the rings depends very loosely on their number, and the spacing lattice, for that matter, and is primarily determined by the optical thickness of a ring. The calculated values of θ for cell variants, as presented in the figures are brought together in Table VII .

The inner fourth ring is so hardly screened that its addition does not affect θ, particularly at larger spacings when the thermal neutron generation in the internal cavity does not matter.

Table VII data were employed to analyse the critical experiments and proved rather benefitial for the agreement between the calculated and experimental data within the framework of few-group models.

REFERENCES

I. Vladimorov V.S. "Computation Mathematics" , 1, 3 (1958).

373

2. Rightmeier R.D. Differential methods of Marginal Problems Solutions. Moscow, Foreign Literature Publ. House, 1962.
3. Lusternik L.A. "Comments on Numerical Marginal Problem Solutions of the Laplase Equation and Eigenvalue Calculations by Grid Methods". Math. Inst. Papers of the Ac. of Sc., USSR, 1947, 20, 49-64.
4. Amouyal A., Benoist P., Horowitz J. "Nouvelle Methode de Determination du Facteur d'Utilisation Thermique d'une Cellule". J. Nucl. Energy, 6, 79 (1957).
5. Mostovoy V.I. et al. Neutron Spectrum Measuring in Uranium - Water and Uranium-Monoisopropildifenile. "Atomic Energy", 13, is. 6, 547 (1962).
6. Martchuk G.I. et al. Slow Neutron Spectrum Calculations. Papers of Third International Conference on Peaceful Use of Atomic Energy. Geneva. 1964.
7. Martchuk G.I. et al. Slow Neutron Spectrum Calculation Methods . Atomic Energy, 13, issue 6, 534 (1962).
8. Feinberg S.M. et al. Fuel Burnout in Pressurised water Power Reactors and Uranium-Water Lattice Experiments. Papers of the Second International Conference on Peaceful Use of Atomic Energy. (Geneva, 1956). Rep. P/2145.
9. Honeck H.C. The Calculation of the Thermal Utilisation and Disadvantage Factor in Uranium- Water Lattices. Light Water Lattices, Technical Report Series 12, Int.At. En. Agency, Vienna, 1962.
10. Hughes D.J., Schwartz R.B. Neutron Cross Sections, BNL-325, Second Ed., 1958.

1	2	3	4	5
1.5	0.9140	0.9228	0.9229	0.9245
2.0	0.8884	0.8985	0.8991	0.9011
3.0	0.8389	0.8512	0.8529	0.8554
4.0	0.7921	0.8060	0.8087	0.8116

TABLE V

The Effect of Changing $T_{n.g.}$ upon θ

	Four Rings	Two Rings
"The Exact Calculation"	0.5741	0.8499
$T_{n.g.}$ = const.	0.5969	0.8570

TABLE VI

The Burnout and Changes of $\bar{\Phi}$ in the rings

Average Uranium -235 Burnout	Middle Ring	Inner Ring
0	0.5038	0.3081
25%	0.5860	0.3742
50%	0.6881	0.4674

TABLE VII

Values θ for Ring Channel Cells

Cell Radius, cm	Two Rings	Three Rings	Four Rings
2.625	0.850	0.875	0.879
4.725	0.562	0.574	0.574

373

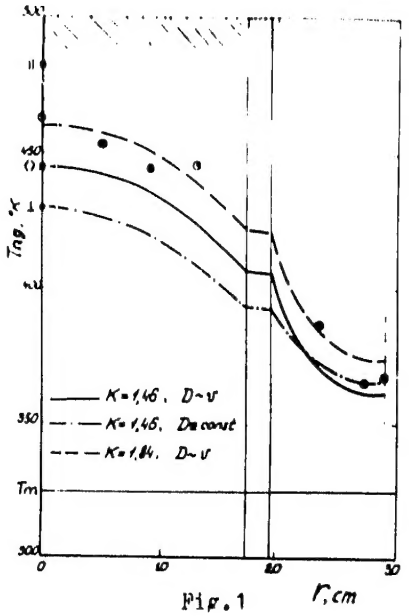

Fig. 1

Neutron gas temperature distribution in the cylindrical cell

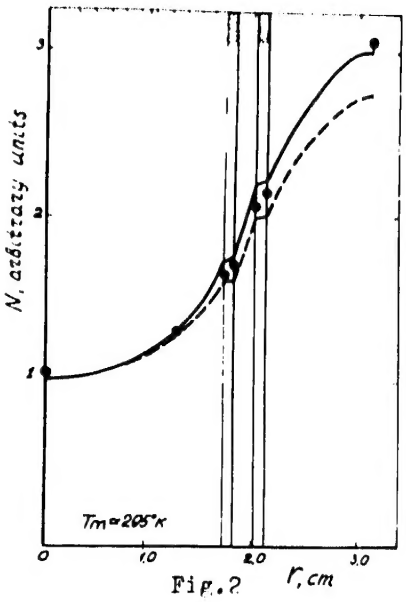

Fig. 2

Neutron integral density distribution in the cylindrical cell

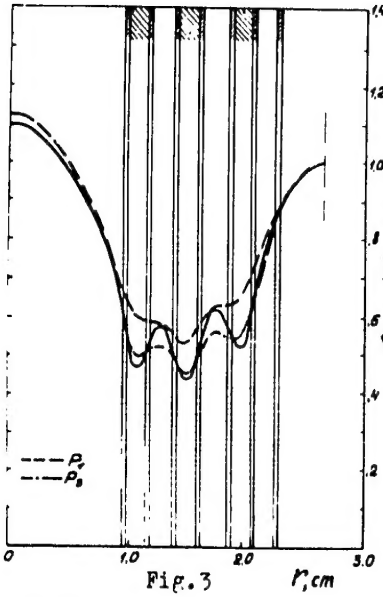

Fig. 3

Comparison of the kinetic, P_3- and P_1-calculation of cell with a three ring channel (one-velocity approximation)

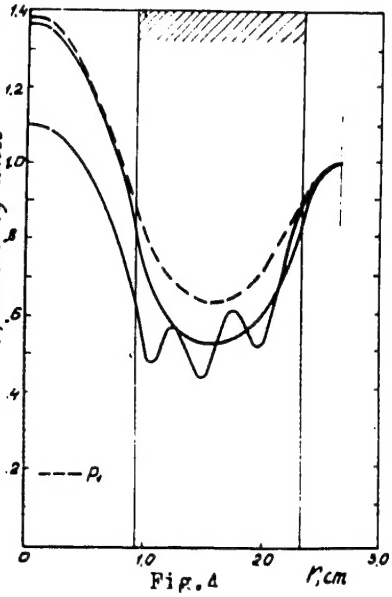

Fig. 4

Comparison of the kinetic cell calculation results with a three ring channel (Fig. 3) and the cell'model calculation

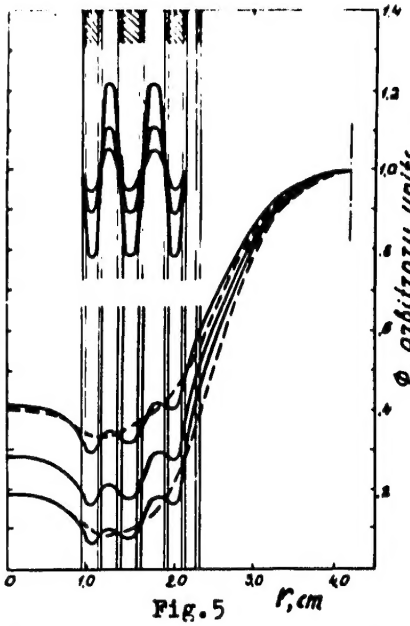

Fig.5

The effect of ring "blackness" on the neutron flux(one-velocity approximation).Dotted line denotes the P_1-calculation of a single-zone model

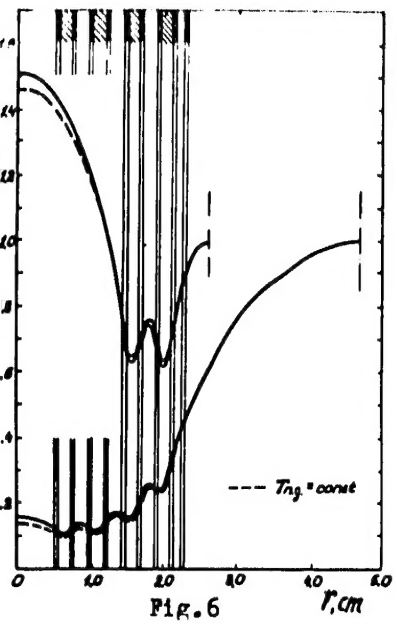

Fig.6

The effect of neutron gas temperature distribution on the equation solution

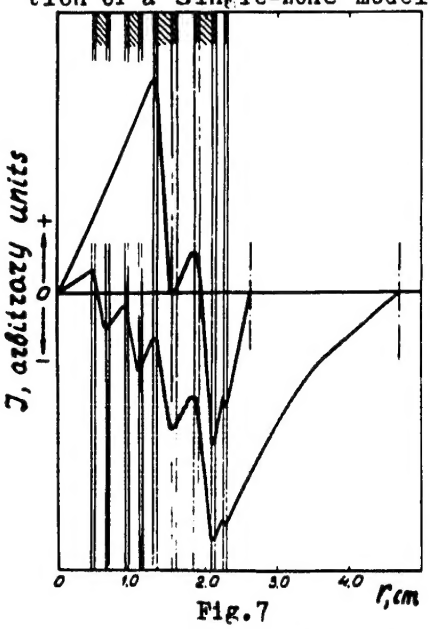

Fig.7

The J current distribution in cells with two- and four-ring channels(See the fluxes in fig.6)

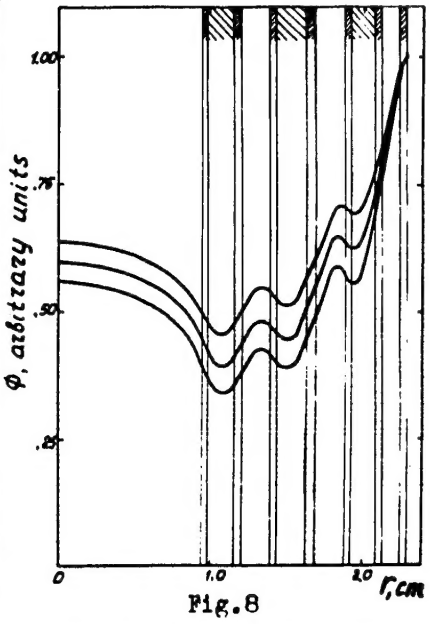

Fig.8

The neutron flux changes due to the three ring channel burnout

373.

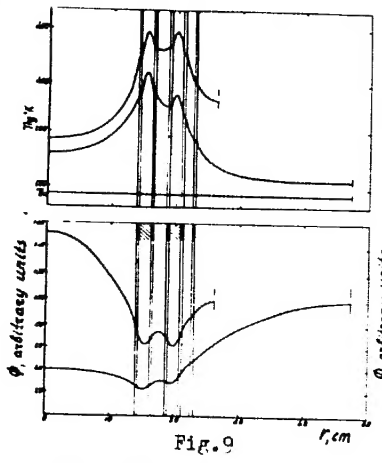

Fig.9

The neutron gas temperature and neutron flux distributions along the two ring channel cell radius

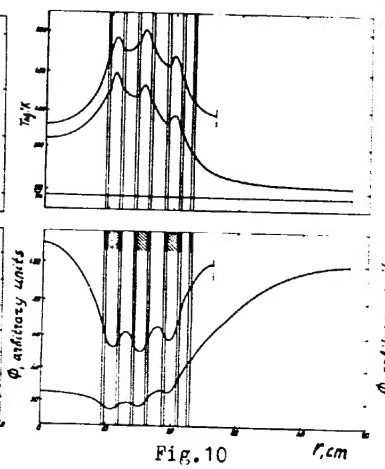

Fig.10

The neutron gas temperature and neutron flux distributions along the three ring channel cell radius

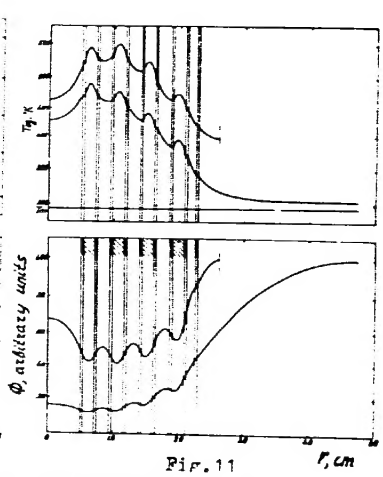

Fig.11

The neutron gas temperature and neutron flux distributions along the four ring channel cell radius